Condensed-phase nitric acid in a tropical subvisible cirrus cloud

P. J. Popp,[1,2] T. P. Marcy,[1,2] L. A. Watts,[1,2] R. S. Gao,[1] D. W. Fahey,[1] E. M. Weinstock,[3] J. B. Smith,[3] R. L. Herman,[4] R. F. Troy,[4] C. R. Webster,[4] L. E. Christensen,[4] D. G. Baumgardner,[5] C. Voigt,[6] B. Kärcher,[6] J. C. Wilson,[7] M. J. Mahoney,[4] E. J. Jensen,[8] and T. P. Bui[8]

Received 27 August 2007; revised 9 November 2007; accepted 28 November 2007; published 28 December 2007.

[1] In situ observations in a tropical subvisible cirrus cloud during the Costa Rica Aura Validation Experiment on 2 February 2006 show the presence of condensed-phase nitric acid. The cloud was observed near the tropopause at altitudes of 16.3–17.7 km in an extremely cold (183–191 K) and dry (<5 ppm H_2O) air mass. Relative humidities with respect to ice ranged from 150–250% throughout most of the cloud. Optical particle measurements indicate the presence of ice crystals as large as 90 μm in diameter. Condensed HNO_3/H_2O molar ratios observed in the cloud particles were 1–2 orders of magnitude greater than ratios observed previously in cirrus clouds at similar HNO_3 partial pressures. Nitric acid trihydrate saturation ratios were 10 or greater during much of the cloud encounter, indicating that HNO_3 may be present in the cloud particles as a stable condensate and not simply physically adsorbed on or trapped in the particles. **Citation:** Popp, P. J., et al. (2007), Condensed-phase nitric acid in a tropical subvisible cirrus cloud, *Geophys. Res. Lett.*, *34*, L24812, doi:10.1029/2007GL031832.

1. Introduction

[2] Subvisible cirrus clouds that form near the tropical tropopause represent an uncertain though potentially significant component in Earth's radiation budget [*McFarquhar et al.*, 2000]. Subvisible cirrus also represent the last opportunity for the removal of water vapor from air entering the stratosphere in the tropics [*Jensen et al.*, 1996]. Owing to the high altitudes and remote locations of subvisible cirrus in the tropics, however, comprehensive in situ observations of these clouds have been limited [*Peter et al.*, 2003]. While cirrus ice particles are known to be effective scavengers of nitric acid (HNO_3) under a range of conditions [*Voigt et al.*, 2007], previous measurements in subvisible cirrus over the western Indian Ocean revealed no evidence of HNO_3 condensed with the ice particles [*Luo et al.*, 2003].

[3] We report here observations of condensed-phase HNO_3 in a tropical subvisible cirrus cloud at high relative humidities with respect to ice (150–250% throughout most of the cloud). These measurements were conducted onboard the NASA WB-57F high-altitude research aircraft as part of the Costa Rica Aura Validation Experiment (CR-AVE). The data are used here to assess the uptake of HNO_3 in subvisible cirrus particles and explore the role of nitric acid trihydrate (NAT) formation in the uptake process.

2. Observations

[4] Condensed-phase HNO_3 was detected in situ with the NOAA chemical ionization mass spectrometer (CIMS) located in the third pallet position of the WB-57F aircraft. The NOAA CIMS methodology for sampling condensed-phase HNO_3 in cirrus clouds has been described in detail elsewhere [*Popp et al.*, 2004]. Briefly, the instrument measures HNO_3 with two independent channels of detection connected to separate forward- and downward-facing inlets. The forward-facing inlet samples both gas- and particle-phase HNO_3. Particles larger than $\sim$1 μm in diameter are inertially stripped from the airstream sampled by the downward-facing inlet, effectively yielding a measure of gas-phase HNO_3. The difference in the signal between the two channels and knowledge of the particle sampling efficiency of the forward-facing inlet allows a determination of the amount of HNO_3 in the condensed phase.

[5] Condensed-phase HNO_3 was observed coincident with a subvisible cirrus cloud on the southbound leg of a WB-57F science flight over the eastern Pacific Ocean on 2 February 2006. The cloud was observed over a geographic extent of approximately 800 km, at latitudes between 7°N and the equator. This flight originated and terminated at Juan Santamaria International Airport in San Jose, Costa Rica (10°N, 84°W). The cloud described here was observed visually by the WB-57F flight crew, but only when viewed horizontally with a long optical path. A real-time display of ice particle number density in the WB-57F cockpit, measured with an optical particle counter, was used to determine a range of flight altitudes to perform porpoising maneuvers through the cloud (Figure 1d). Time series data of HNO_3 mixing ratios observed from the forward and downward CIMS channels are shown in Figure 1a. The presence of condensed-phase HNO_3 is indicated by a significant difference in the HNO_3 mixing ratio observed in the forward and downward CIMS channels (pink highlighted region in Figure 1). The presence of cirrus ice particles is indicated

[1]Chemical Sciences Division, NOAA Earth System Research Laboratory, Boulder, Colorado, USA.
[2]Cooperative Institute for Research in Environmental Sciences, University of Colorado, Boulder, Colorado, USA.
[3]Atmospheric Research Project, Harvard University, Cambridge, Massachusetts, USA.
[4]Jet Propulsion Laboratory, California Institute of Technology, Pasadena, California, USA.
[5]Centro de Ciencias de la Atmosfera, Universidad Nacional Autónoma de México, Mexico City, Mexico.
[6]Institut für Physik der Atmosphäre, Deutsches Zentrum für Luft- und Raumfahrt, Oberpfaffenhofen, Germany.
[7]Department of Engineering, University of Denver, Denver, Colorado, USA.
[8]NASA Ames Research Center, Moffett Field, California, USA.

0094-8276/07/2007GL031832$05.00

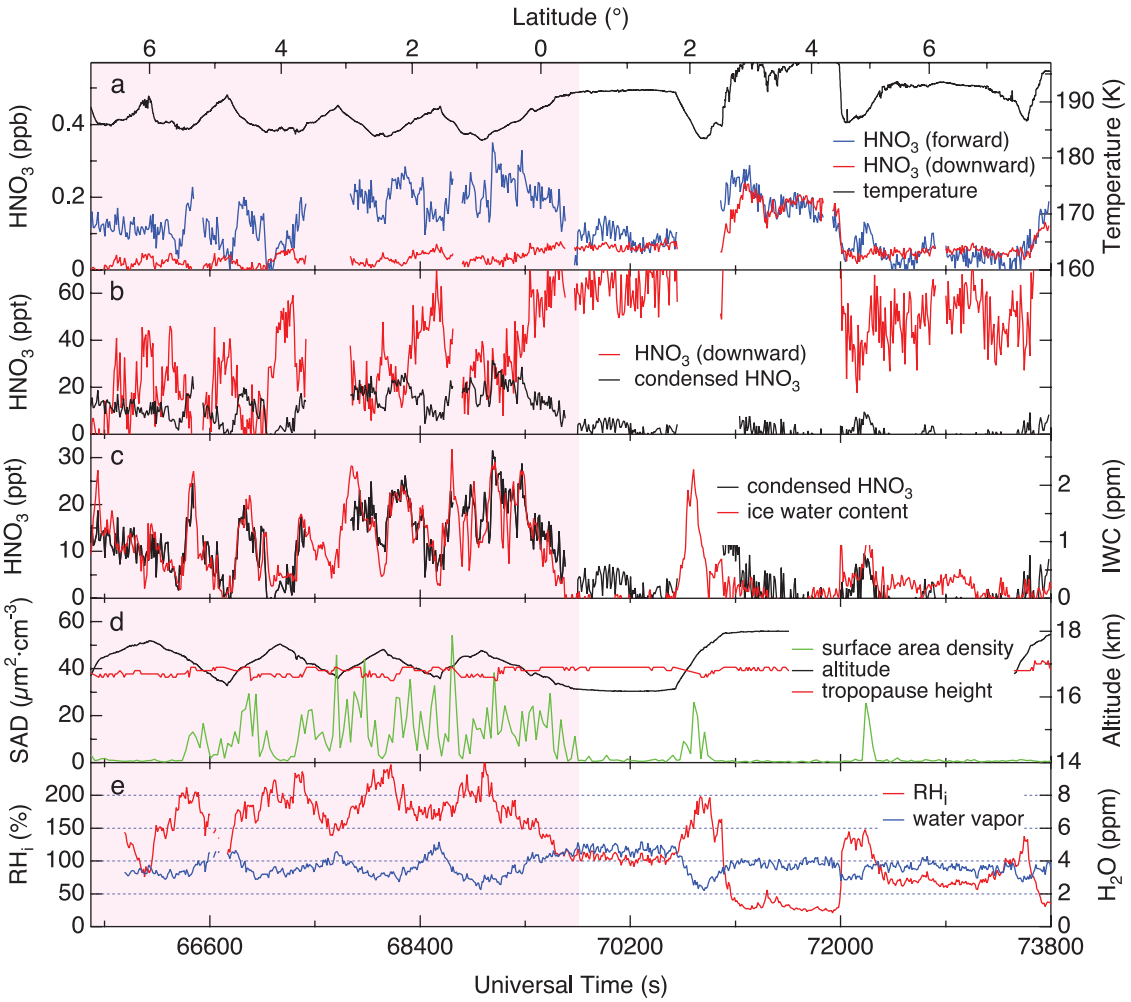

Figure 1. Time series measurements of HNO_3 mixing ratio observed from the forward and downward CIMS channels on the flight of 2 February 2006. The subvisible cirrus cloud was observed in the pink highlighted region. Also shown are ambient temperature [*Scott et al.*, 1990], condensed HNO_3, IWC (calculated as the difference between total water and water vapor [*Webster et al.*, 1994; *May*, 1998]), SAD [*Baumgardner et al.*, 2001], flight altitude, tropopause height [*Denning et al.*, 1989], water vapor [*Weinstock et al.*, 1994], and relative humidity. (a, b, c) Note the change in the HNO_3 scale.

by enhancements in ice water content (IWC) and surface area density (SAD) above background values (Figures 1c and 1d).

[6] The subvisible cirrus cloud was observed at flight altitudes of approximately 16.3–17.7 km. Microwave temperature profiles indicate that the cirrus layer was observed at or slightly higher than the lapse-rate tropopause (Figure 1d). The cold-point tropopause during the cloud encounter occurred approximately 500 m higher than the lapse-rate tropopause, but still within the cloud. Ambient temperatures in this region ranged from 183–191 K (Figure 1a). These low temperatures and ambient water vapor values of 2.3–5.2 ppm correspond to relative humidities with respect to ice of 150–250% throughout most of the cloud (Figure 1e). Measurements in subvisible cirrus during at least one other CR-AVE flight revealed similarly high relative humidities [*Jensen et al.*, 2007]. Gas-phase HNO_3 mixing ratios observed near the tropical tropopause were less than 100 ppt. Despite these low values, the low ambient temperatures caused nitric acid trihydrate (NAT) saturation ratios to be 10 or greater during much of the cloud encounter [*Hanson and Mauersberger*, 1988].

[7] Condensed-phase HNO_3 values, calculated by accounting for the particle sampling efficiency of the CIMS instrument [*Popp et al.*, 2004], exceeded 30 ppt during the cloud encounter (Figures 1b and 1c). Ice water content shows a strong temporal correlation with condensed-phase HNO_3 in the cloud (Figure 1c), consistent with previous measurements in convectively formed subtropical cirrus clouds [*Popp et al.*, 2004]. Measurements in the convective cirrus also showed a strong correlation between condensed-phase HNO_3 and ice particle SAD. Ice particle SADs are derived by integrating particle size distribution and number density measurements from the Cloud, Aerosol, and Precipitation Spectrometer (CAPS) assuming quasi-spherical particles in this size range [*Baumgardner et al.*, 2001]. Ice particle SADs in the cloud were typically less than 50 $\mu m^2 \cdot cm^{-3}$ (Figure 1d), which is in strong contrast to SADs of up to $6 \cdot 10^5$ $\mu m^2 \cdot cm^{-3}$ observed in the convectively-formed cirrus [*Popp et al.*, 2004]. We note that the SAD values observed at the beginning of the cloud encounter

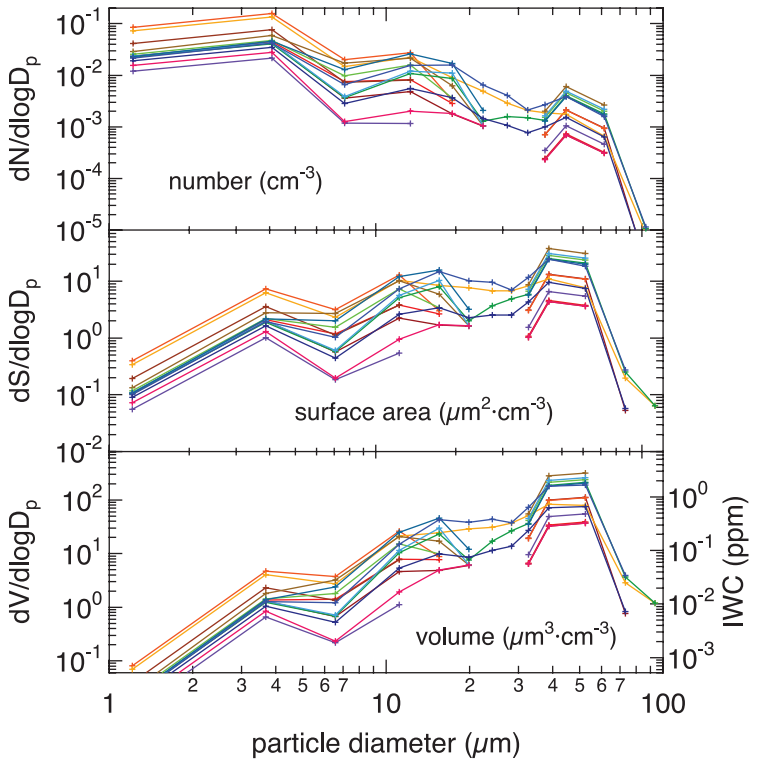

Figure 2. Particle number, surface area, and volume density distributions measured in the subvisible cirrus. Data are shown as 5-minute averages throughout the cloud.

(<66600 UT, Figure 1d) are lower than expected, given the enhanced values of IWC and condensed-phase HNO_3 observed during the same time period (Figure 1c).

[8] Ice particle size distributions reported by the CAPS instrument show the presence of large ice crystals (30–90 μm diameter) in the cloud, as well as a smaller particle mode at 10–20 μm (Figure 2). The size distributions also indicate that the ice particle surface area and volume density, and therefore ice water content, are dominated by the large-particle mode. An ice particle growth model [*Jensen et al.*, 2007] indicates that growth times for the largest particles shown in Figure 2 (90 μm) are ~3–4 hours under conditions observed in the subvisible cirrus cloud. Smaller particles (30 μm) have growth times less than one hour.

3. Discussion

[9] We assume that the sampled particles are composed primarily of ice, with a small molar fraction of HNO_3 contained in the bulk of the particle [*Kärcher and Voigt*, 2006]. The data reported here suggest the observed condensed-phase HNO_3 does not exist as a separate population of NAT particles or STS aerosol. First, condensed-phase HNO_3 exhibits a strong temporal correlation with ice water content in the cloud and was only observed in the presence of cirrus particles, as indicated by enhancements in both ice water content and ice particle surface area density (Figure 1). Second, a population of STS aerosols cannot grow to sizes large enough to produce the differential response shown by the CIMS instrument in Figure 1a. Particles smaller than approximately 1 μm in diameter are neither enhanced in the forward-facing CIMS inlet nor inertially stripped from the airstream sampled by the downward-facing inlet. Finally, maximum values of ice water content observed in the cloud (~2.5 ppm, Figure 1c) can be accounted for by the large (30–90 μm) ice particle mode observed by the CAPS instrument (Figure 2).

[10] Results from the Aerosol Inorganics Model (AIM) [*Carslaw et al.*, 1995] indicate that, under ambient conditions typical for the observed cloud (with ice formation inhibited in the model run to simulate ice supersaturation), gas-phase HNO_3 will be depleted at temperatures less than approximately 191 K should NAT form (Figure 3). The model also indicates that the background sulfate aerosol can take up a substantial fraction of the available HNO_3 at temperatures less than approximately 188 K, resulting in the production of a supercooled ternary solution (STS) of water, sulfuric acid and HNO_3. At temperatures less than 186 K, essentially all of the ambient HNO_3 can be partitioned into the STS phase. We note, however, that the AIM describes HNO_3 partitioning under equilibrium conditions and does not account for the uptake of HNO_3 by cirrus ice crystals. The observations reported here indicate that HNO_3 partitions into the ice phase when present, sometimes completely, despite the fact that NAT or STS aerosols are also thermodynamically stable. These results are consistent with numerical simulations of a polar cirrus cloud that indicate HNO_3 will be driven from the liquid aerosol and incorporated in cirrus particles as soon as ice forms [*Kärcher*, 2005].

[11] Microphysical modeling studies together with in situ observations provide evidence that HNO_3 can be trapped and subsequently buried in growing ice particles under

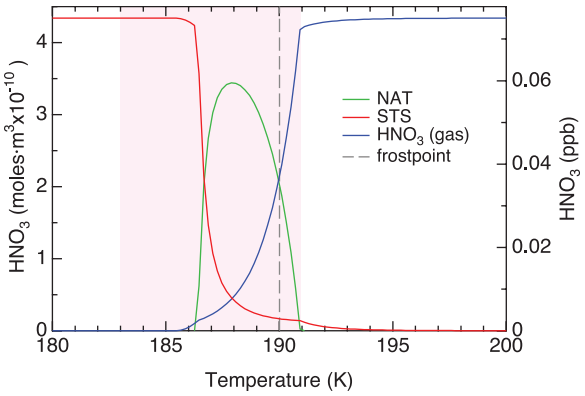

Figure 3. HNO_3 partitioning in the tropical lower stratosphere calculated by the Aerosol Inorganics Model (AIM). Model inputs, typical of conditions observed in the subvisible cirrus cloud, were 75 ppt HNO_3, 3.5 ppm H_2O, and 0.25 ppbm H_2SO_4 [*Wilson et al.*, 1992]. The temperature range observed in the subvisible cirrus is shown by the region highlighted in pink.

conditions typical of the tropical tropopause [*Kärcher and Voigt*, 2006; *Voigt et al.*, 2006; *Voigt et al.*, 2007]. The trapping process is fundamentally controlled by the HNO_3 residence time on the ice surface and the particle growth rate [*Kärcher and Basko*, 2004]. As a result, the efficiency of the trapping process increases with decreasing temperature and increasing relative humidity. The HNO_3 content in cirrus particles can be expressed as the condensed HNO_3/H_2O molar ratio [*Voigt et al.*, 2006]. The observed HNO_3/H_2O ratios in the subvisible cirrus reported here are 1–2 orders of magnitude greater than ratios previously observed in cirrus clouds at similar HNO_3 partial pressures (Figure 4). It's reasonable to speculate that these high ratios result from the low temperatures (183–191 K) and the associated high RH_i values (150–250%) in the cloud. Under such conditions, trapping theory predicts that the maximum condensed HNO_3/H_2O ratio in a cirrus particle is approximately one quarter of the ambient gas-phase HNO_3/H_2O ratio [*Kärcher and Voigt*, 2006]. This limitation of less than unity is due to the effective gas phase diffusion coefficients of HNO_3 and H_2O. Since the mean condensed HNO_3/H_2O ratio reported here ($1.4 \cdot 10^{-5}$, Figure 4) is ~0.25 times the ambient HNO_3/H_2O ratio at higher altitudes (~18 km) where these particles nucleate (Figure 1, 71100 UT), these results indicate very efficient trapping of HNO_3 in the observed cloud. These observations are consistent with laboratory measurements that reveal enhanced and long-term HNO_3 uptake on growing ice films at RH_i values greater than 100% (compared to static ice films), indicative of the trapping of HNO_3 in the film [*Ullerstam and Abbatt*, 2005]. It is also worth noting that the HNO_3 dissolved in ice at equilibrium, extrapolated from laboratory measurements at higher temperatures and HNO_3 partial pressures [*Thibert and Dominé*, 1998], is approximately an order of magnitude too low to produce the condensed HNO_3/H_2O molar ratios in the cloud reported here (Figure 4). We conclude, therefore, that the condensed HNO_3 we observe is truly trapped in the particle and not simply dissolved in the ice.

[12] Water vapor was measured with multiple instruments onboard the WB-57F during CR-AVE. Recently, the accuracy of water vapor measurements at low mixing ratios has been under careful scrutiny because significant differences have been reported between various instruments during previous measurement campaigns. The water vapor data shown in Figure 1 are provided by the Harvard Water Vapor (HWV) instrument using a Lyman-α fluorescence detection scheme [*Weinstock et al.*, 1994]. The reported accuracy of the HWV instrument was ±15% at water vapor mixing ratios less than 10 ppm during the flight on 2 February 2006. While there was no significant difference between the HWV and Integrated Cavity Output Spectroscopy (ICOS) instruments [*Sayres*, 2006] during this flight (data not shown), the ICOS measurements were ~0.5 ppm lower than the HWV measurements on at least one other CR-AVE flight [*Jensen et al.*, 2007]. The reported accuracy for the ICOS instrument is ±5%, with a potential bias of 0.25 ppm. Thus, a difference of 0.5 ppm does not represent a significant discrepancy between the two instruments. At the low water vapor mixing ratios observed in the subvisible cirrus cloud, a difference in water vapor of 0.5 ppm represents a decrease of approximately 25% in the calculated RH_i. We conclude, therefore, that water vapor is highly supersaturated throughout most of the cloud (RH_i of at least 125–225%) regardless of the water vapor measurement chosen for this analysis.

[13] Finally, we note that the cloud described here was highly supersaturated with respect to NAT. Measurements in contrail cirrus at temperatures less than T_{NAT} have fueled speculation that HNO_3 serves to increase the relative humidity with respect to ice in low-temperature cirrus clouds via the formation of NAT-like hydrates on the particle surface [*Gao et al.*, 2003]. With the simultaneous observation of condensed-phase HNO_3 and high relative humidities in the cloud reported here, it seems reasonable to speculate that HNO_3 uptake by subvisible cirrus particles might play an important role in the water vapor budget near the tropopause [*Gao et al.*, 2003]. It is also worth noting

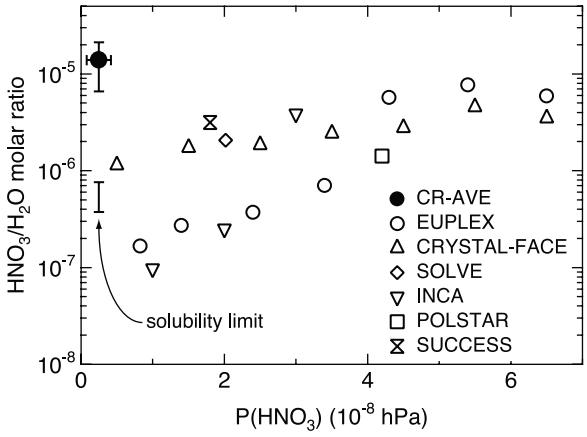

Figure 4. Relationship between the HNO_3/H_2O molar ratio in cirrus particles and the HNO_3 partial pressure in the cloud from various airborne field campaigns. All data except CR-AVE taken from *Voigt et al.* [2006]. The solubility limit of HNO_3 in ice is shown for the range of temperatures observed in the cloud (183–191 K).

that NAT formation on the particle surface is likely to increase the HNO_3 residence time on the particle (i.e. decrease the rate of escape from the surface) and further enhance the HNO_3 trapping process [*Kärcher and Voigt*, 2006].

[14] **Acknowledgments.** The authors wish to thank the air and ground crews of the NASA WB-57F aircraft. Access to the online Aerosol Inorganics Model by S. L. Clegg, P. Brimblecombe, and A. S. Wexler at http://www.aim.env.uea.ac.uk/aim/aim.html is greatly appreciated. This work was partially supported by the NASA Upper Atmospheric Research Program and NOAA Atmospheric Chemistry and Climate Program. Work performed at the Jet Propulsion Laboratory, California Institute of Technology, was done under contract with NASA.

References

Baumgardner, D., et al. (2001), The cloud, aerosol and precipitation spectrometer: A new instrument for cloud investigations, *Atmos. Res.*, *59–60*, 251–264.

Carslaw, K. S., S. L. Clegg, and P. Brimblecombe (1995), A thermodynamic model for the system of HCl-HNO_3-H_2SO_4-H_2O, including solubilities of HBr, from <200 K to 328 K, *J. Phys. Chem.*, *99*, 11,557–11,574.

Denning, R. F., S. L. Guidero, G. S. Parks, and B. L. Gary (1989), Instrument description of the Airborne Microwave Temperature Profiler, *J. Geophys. Res.*, *94*, 16,757–16,765.

Gao, R. S., et al. (2003), Evidence that ambient nitric acid increases relative humidity in low-temperature cirrus clouds, *Science*, *303*, 516–520.

Hanson, D., and K. Mauersberger (1988), Laboratory studies of the nitric acid trihydrate: Implications for the South polar stratosphere, *Geophys. Res. Lett.*, *15*, 855–858, doi:10.1029/88GL00209.

Jensen, E. J., O. B. Toon, L. Pfister, and H. B. Selkirk (1996), Dehydration of the upper troposphere and lower stratosphere by subvisible cirrus clouds near the tropical tropopause, *Geophys. Res. Lett.*, *23*, 825–828, doi:10.1029/96GL00722.

Jensen, E. J., et al. (2007), Formation of large ($\sim$100 μm) ice crystals near the tropical tropopause, *Atmos. Chem. Phys. Discuss.*, *7*, 6293–6327.

Kärcher, B. (2005), Supersaturation, dehydration and denitrification in Arctic cirrus, *Atmos. Chem. Phys.*, *5*, 1757–1772.

Kärcher, B., and M. M. Basko (2004), Trapping of trace gases in growing ice crystals, *J. Geophys. Res.*, *109*, D22204, doi:10.1029/2004JD005254.

Kärcher, B., and C. Voigt (2006), Formation of nitric acid/water ice particles in cirrus clouds, *Geophys. Res. Lett.*, *33*, L08806, doi:10.1029/2006GL025927.

Luo, B. P., et al. (2003), Dehydration potential of ultrathin clouds at the tropical tropopause, *Geophys. Res. Lett.*, *30*(11), 1557, doi:10.1029/2002GL016737.

May, R. D. (1998), Open-path, near-infrared tunable diode laser spectrometer for atmospheric measurements of H_2O, *J. Geophys. Res.*, *103*(D15), 19,161–19,172.

McFarquhar, G. M., et al. (2000), Thin and subvisual tropopause tropical cirrus: Observations and radiative impacts, *J. Atmos. Sci.*, *57*, 1841–1853.

Peter, T., et al. (2003), Ultrathin Tropical Tropopause Clouds (UTTCs): I. Cloud morphology and occurrence, *Atmos. Chem. Phys.*, *3*, 1083–1091.

Popp, P. J., et al. (2004), Nitric acid uptake on subtropical cirrus cloud particles, *J. Geophys. Res.*, *109*, D06302, doi:10.1029/2003JD004255.

Sayres, D. S. (2006), New techniques for accurate measurement of water and water isotopes, Ph.D. thesis, Harvard Univ., Cambridge, Mass.

Scott, S. G., et al. (1990), The meteorological measurement system on the NASA ER-2 aircraft, *J. Atmos. Oceanic Technol.*, *7*, 525–540.

Thibert, E., and F. Dominé (1998), Thermodynamics and kinetics of the solid solution of HNO_3 in ice, *J. Phys. Chem. B*, *102*, 4432–4439, doi:10.1021/jp980569.

Ullerstam, M., and J. P. D. Abbatt (2005), Burial of gas-phase HNO_3 by growing ice surfaces under tropospheric conditions, *Phys. Chem. Chem. Phys.*, *7*, 3596–3600.

Voigt, C., H. Schlager, H. Ziereis, B. Kärcher, B. P. Luo, C. Schiller, M. Krämer, P. J. Popp, H. Irie, and Y. Kondo (2006), Nitric acid in cirrus clouds, *Geophys. Res. Lett.*, *33*, L05803, doi:10.1029/2005GL025159.

Voigt, C., et al. (2007), In situ observations and modeling of small nitric acid-containing ice crystals, *Atmos. Chem. Phys.*, *7*, 3373–3383.

Webster, C. R., et al. (1994), Aircraft (ER-2) laser infrared absorption spectrometer (ALIAS) for in-situ stratospheric measurements of HCl, N_2O, CH_4, NO_2, and HNO_3, *Appl. Opt.*, *33*, 454–472.

Weinstock, E. M., et al. (1994), New fast-response photofragment fluorescence hygrometer for use on the NASA ER-2 and the Perseus remotely piloted aircraft, *Rev. Sci. Instrum.*, *65*, 3544–3554.

Wilson, J. C., M. R. Stolzenburg, W. E. Clark, M. Loewenstein, G. V. Ferry, K. R. Chan, and K. K. Kelly (1992), Stratospheric sulfate aerosol in and near the Northern Hemisphere polar vortex: The morphology of the sulfate layer, multimodal size distributions, and the effect of denitrification, *J. Geophys. Res.*, *97*(D8), 7997–8013.

D. G. Baumgardner, Centro de Ciencias de la Atmosfera, Universidad Nacional Autónoma de México, Circuito Exterior s/n, Cuidad Universitaria, Mexico City, Mexico City D. F. 04150, México.

T. P. Bui and E. J. Jensen, NASA Ames Research Center, Moffett Field, CA 94035, USA.

L. E. Christensen, R. L. Herman, M. J. Mahoney, R. F. Troy, and C. R. Webster, Jet Propulsion Laboratory, California Institute of Technology, Pasadena, CA 91109, USA.

D. W. Fahey, R. S. Gao, T. P. Marcy, P. J. Popp, and L. A. Watts, Chemical Sciences Division, NOAA Earth System Research Laboratory, 325 Broadway R/AL6, Boulder, CO 80305, USA. (peter.j.popp@noaa.gov)

B. Kärcher and C. Voigt, Institut für Physik der Atmosphäre, Deutsches Zentrum für Luft- und Raumfahrt, Oberpfaffenhofen, Postfach 1116, D-82230 Wessling, Germany.

J. B. Smith and E. M. Weinstock, Atmospheric Research Project, Harvard University, Cambridge, MA 02138, USA.

J. C. Wilson, Department of Engineering, University of Denver, Denver, CO 80208, USA.